Materials Advances

Accepted Manuscript

This article can be cited before page numbers have been issued, to do this please use: P. D. Dewale and N. Dey, *Mater. Adv.*, 2026, DOI: 10.1039/D6MA00118A.

ROYAL SOCIETY OF CHEMISTRY

rsc.li/materials-advances

DOI: 10.1039/D6MA00118A

Counter-Ion-Regulated Fluoride Sensing by a Silyl-Protected, Highly Conjugated Molecular Derivative: From On-Field Analysis to Quantification of Nerve Gas Simulants

Prashant. D. Dewale, and Nilanjan Dey[a]*
[a]Department of Chemistry, Birla Institute of Technology and Science Pilani, Hyderabad campus, Hyderabad, Telangana 500078, India
Email: nilanjandey.iisc@gmail.com, nilanjan@hyderabad,bits-pilani.ac.in

ABSTRACT

We report the design and synthesis of a π-conjugated electron–rich molecular system bearing silyl-protected phenolic units and flexible oxyethylene linkers, engineered for selective fluoride sensing in semi-aqueous environments. The probe operates via a fluoride-triggered desilylation mechanism, via fluoride-triggered desilylation. This transformation induces a distinct bathochromic shift in absorption and a ratiometric fluorescence response, accompanied by aggregation-assisted stabilization of a low-energy emissive state in the presence of weakly coordinating counter-ions. Spectroscopic and DFT studies support the sensing mechanism. The probe exhibits high selectivity for fluoride over competing anions, with sensitivity strongly governed by solvent composition and pH. Importantly, the system enables quantitative fluoride detection in real water samples and functions in a portable paper-strip format. Under basic conditions, it further detects diisopropyl fluorophosphate through in situ fluoride release, highlighting a dual-use platform for environmental monitoring and chemical defense applications.

KEYWORDS: Silylated OPV derivatives; Fluoride sensing; Counter ion-directed assembly; Nerve gas stimulants; On-location detection

HIGHLIGHTS

- Water-soluble Oligo (p-phenylene vinylene) (OPV) fluoride probe
- Desilylation-driven change in ICT state and self-assembly behavior
- Multi-parametric analysis of Nerve gas agents in aqueous medium
- Screening of Real water sample and paper strip-based detection system

INTRODUCTION

Oligo (p-phenylene vinylene) (OPV)–based systems have garnered widespread attention in advanced optical sensing because their extended π-conjugated backbones intrinsically amplify electronic and photophysical responses to external perturbations.[1] The delocalized π-electron framework facilitates efficient long-range intramolecular charge transfer (ICT), as reflected in large molar extinction coefficients and pronounced analyte-induced spectral shifts. Consequently, even subtle chemical transformations or binding events at terminal recognition sites can propagate through the entire conjugated scaffold, producing substantial changes in absorption and emission outputs, a phenomenon often referred to as molecular-derivative-assisted signal amplification.[2] OPVs further exhibit superior photostability, as delocalization of excited-state energy suppresses photo-oxidative degradation and photobleaching pathways commonly encountered in small, localized fluorophores.[3] Their modular architecture allows precise tuning of conjugation length, donor strength, and side-chain polarity, enabling controlled modulation of HOMO–LUMO gaps, excited-state lifetimes, and radiative versus non-radiative decay processes. In addition, OPV scaffolds readily undergo controlled self-assembly via π–π stacking and van der Waals interactions, facilitating aggregation-assisted sensing and access to low-energy emissive states with enhanced sensitivity.[4, 5] These

collective attributes establish OPV-based probes as robust, highly sensitive, and environment-tolerant platforms for optical sensing in complex media.[6]

Considering these advantages, herein we employ a highly conjugated silyl-protected OPV derivative as an efficient fluoride-responsive optical probe (Figure 1a). Broadly, the current fluoride sensing relies on mechanisms based on interaction (hydrogen bonding), reaction (desilylation or cleavage), and demetallation[7, 8]. The high flexibility in designing the probe with silyl groups and the widely explored desilylation mechanism offer high selectivity and a strong driving force. The sensing mechanism is governed by fluoride-induced desilylation, which triggers a pronounced modulation of the intramolecular charge transfer (ICT) characteristics of the OPV backbone.[7, 9, 10] Upon fluoride-induced desilylation, the electronic structure undergoes a marked transformation. Formation of phenoxide (O^-) groups significantly increases the electron-donating strength of the terminal units, effectively converting the molecule into a highly polarized donor–π–donor$^-$ (D–π–D$^-$) system. This induces an internal push–pull electronic effect even in the absence of a conventional acceptor, resulting in pronounced intramolecular polarization. Notably, for the first time, we systematically elucidate the critical role of counter ions in fluoride sensing, demonstrating how organic and inorganic fluoride sources can be distinctly differentiated through counter-ion–regulated self-assembly behavior. While fluoride delivered via tetrabutylammonium fluoride (TBAF) promotes loose ion pairing and aggregation of the desilylated phenoxide species, leading to stabilized low-energy emissive states, fluoride from potassium fluoride (KF) forms tight contact ion pairs that suppress supramolecular assembly and limit ICT stabilization. This counter-ion-dependent aggregation mechanism provides a unique and previously unexplored dimension in OPV-based fluoride sensing, enabling discrimination between organic and inorganic fluoride sources beyond conventional intensity-based detection.

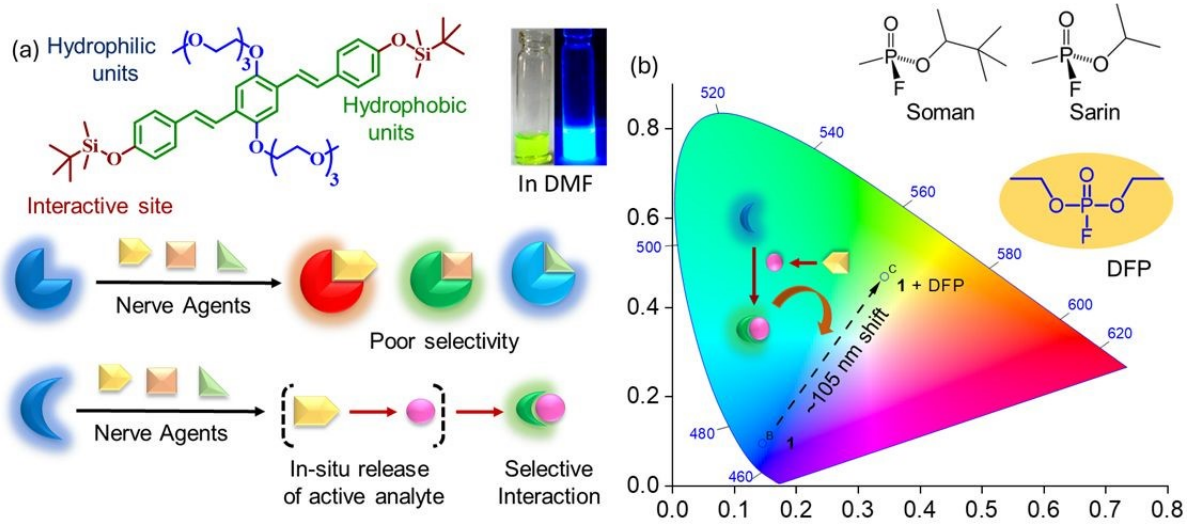

Figure 1. (a) Structure of the compound involved in the present study. (b) Chromogenic response of compound 1 towards DFP via chemodosimetric interaction.

On the other hand, detection of diisopropyl fluorophosphate (DFP) and related nerve agents is of paramount importance owing to their extreme neurotoxicity, rapid onset of action, and persistent threat in both military and civilian contexts.[11-13] DFP is widely employed as a simulant for G-series nerve agents because it shares a common P–F bond and acetylcholinesterase inhibition pathway, making it highly relevant for chemical defense research and sensor development (Figure 1b).[14] However, reliable sensing of DFP remains particularly challenging due to its relatively low intrinsic reactivity, slow hydrolysis kinetics under neutral conditions, and lack of strong spectroscopically active functional groups.[15]

View Article Online
DOI: 10.1039/D6MA00118A

Consequently, the number of reported sensors for DFP is significantly lower than for other organophosphates such as diethyl chlorophosphate (DCP) and diethyl cyanophosphonate (DCNP), which contain more labile P–Cl or P–CN bonds and readily undergo nucleophilic substitution, enabling direct interaction with nucleophilic or hydrogen-bonding probes.[16] In contrast, DFP requires either enzymatic activation or base-catalyzed hydrolysis to release fluoride ions, limiting the applicability of conventional reaction-based sensing strategies.[17] In the present work, we address this challenge by exploiting a fluoride-responsive, silyl-protected OPV scaffold and intentionally operating under mildly basic conditions to promote controlled hydrolysis of DFP. The in situ–generated fluoride ions trigger desilylation, leading to quantifiable and time-resolved optical changes, thereby enabling both detection and quantification of DFP through an indirect yet highly selective fluoride-mediated signaling pathway.[7, 18, 19]

RESULTS AND DISCUSSION

Design and synthesis of probe molecule: Compound 1 was conveniently prepared via a stepwise etherification and silylation sequence, ensuring high solubility, chemical stability, and modular functionality. The molecule features a donor-enriched π-conjugated scaffold symmetrically functionalized with tert-butyldimethylsilyl (TBDMS)-protected phenolic groups (latent donors) and triethylene glycol (TEG)-substituted alkoxy units that contribute electron density via a +M effect. Within this framework, the central OPV backbone is comparatively electron-deficient and behaves as a weak acceptor due to conjugation with these multiple donor groups, rather than from any intrinsic electron-withdrawing character. The central chromophoric backbone incorporates an electron-deficient core flanked by extended π-systems containing alkoxy linkers, which facilitate a weak intramolecular charge transfer (ICT) upon electronic excitation. The inclusion of flexible triethylene glycol (TEG) linkers enhances solvation and dispersibility in mixed organic–aqueous media, a critical factor for maintaining sensor performance under semi-aqueous conditions.[20] Structurally, the TBDMS groups act as both the reactive fluoride-responsive sites and hydrophobic barriers, balancing reactivity and stability in complex media.[21] This rational molecular architecture thus enables compound 1 to detect not only direct fluoride sources (e.g., TBAF or KF) but also fluoride generated in situ from the hydrolysis of organophosphorus nerve-agent simulants such as DFP, making it a powerful, dual-function probe for environmental fluoride monitoring and chemical defense applications.[22, 23]

Detection of fluoride ions in solution phase: Considering the presence of an anion-responsive terminal functional group, we initially investigated the interaction of compound 1 with various anions in an aqueous medium (pH 7.5 buffer). Upon addition of different anions (~2 mM), including fluoride, no noticeable change in either visible color or fluorescence emission was observed, even after prolonged incubation (>1 h). The UV–visible spectra of compound 1 recorded in the presence of these anions showed only negligible spectral perturbations (Figure S2a). Notably, in the case of fluoride ions, a very weak and broad charge-transfer band appeared at longer wavelengths (>450 nm), indicating a marginal interaction between fluoride and the probe under purely aqueous conditions. Similarly, fluorescence spectra recorded under identical conditions revealed that among all the tested anions, only fluoride induced a modest quenching of fluorescence intensity (~1.2-fold), while other anions produced essentially no response (Figure S2b). These results suggest that compound 1 is capable of selectively recognizing fluoride ions even in water; however, the extremely weak optical responses render the system unsuitable for reliable quantitative analysis in a purely aqueous medium.

View Article Online
DOI: 10.1039/D6MA00118A

We attributed this poor sensing performance primarily to the pronounced self-aggregation of compound 1 in water.[24] This hypothesis was further supported by solvent-dependent UV-visible and fluorescence studies. In organic solvents, UV-visible spectra of compound 1 showed absorption maxima ~342 nm, while in water, a rather broad spectrum was witnessed with maxima slightly red-shifted (~350 nm) (Figure S3a). Similarly, compound 1 exhibited strong fluorescence with two well-resolved emission bands at 442 and 465 nm, characteristic of monomeric emissive species in organic medium (Figure S3b). In contrast, when recorded in water, the fluorescence intensity decreased substantially, and the emission spectrum became broad with two red-shifted maxima at 455 and 475 nm. Such spectral broadening and red shift (in both absorption and fluorescence modes) are indicative of aggregation-induced excited-state interactions, which likely suppress effective analyte binding and signal transduction.[25, 26] The self-assembly of compound 1 in the aqueous medium was also evident from DLS studies, where formation of colloidal particles with average hydrodynamic diameters ~150 ± 8 nm (Figure S4). Therefore, to minimize aggregation effects while maintaining sufficient fluoride reactivity, we selected organic–water mixed solvent systems for subsequent anion-sensing investigations. This approach allowed better control over probe dispersion, fluoride availability, and photophysical responsiveness, ultimately enabling more pronounced and quantifiable optical changes upon fluoride interaction.

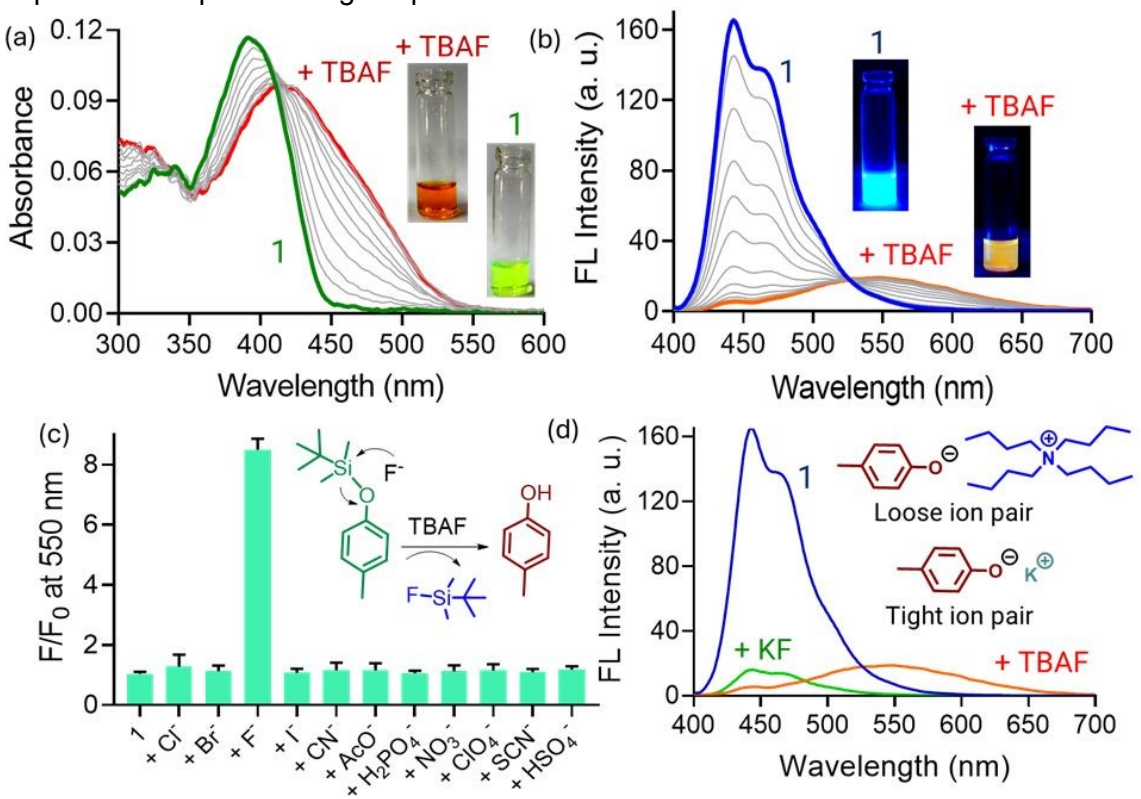

Figure 2. (a) UV-visible titration of compound 1 (10 μM) with TBAF (0 – 1 mM) in DMF-H_2O (9:1, pH 7.5 buffer) medium. (b) Fluorescence titration of compound 1 (10 μM, λex = 390 nm) with TBAF (0 – 1 mM) in DMF-H_2O (9:1, pH 7.5 buffer) medium. (c) Changes in fluorescence intensity of compound 1 (10 μM, λex = 390 nm) at 550 nm upon addition of various anions (1 mM) in DMF-H_2O (9:1, pH 7.5 buffer) medium. (d) Fluorescence spectra of compound 1 (10 μM, λex = 390 nm) with TBAF and KF (1 mM) in DMF-H_2O (9:1, pH 7.5 buffer) medium.

The absorption spectrum of compound 1 showed the presence of two bands at ~330 nm (due to a π–π* transition) and ~392 nm (due to intramolecular charge transfer) respectively in a DMF–H_2O (9:1) mixture medium (Figure 2a).[27, 28] The addition of TBAF resulted in a red shift in absorption maxima to 415 nm with a broad charge-transfer absorption at the longer

View Article Online
DOI: 10.1039/D6MA00118A

wavelength region (450–530 nm), attributing to fluoride-triggered desilylation and subsequent generation of a strongly electron-donating phenoxide moiety, which enhances the ICT character of the molecule.[29] This electronic reorganization resulted in a visible solution color change from light green to dark yellow. UV–visible titration studies showed a concentration-dependent gradual increase in absorbance at the 470 nm region (~2.2-fold) with concomitant diminution at the 392 nm band. The presence of isosbestic points at 337 and 408 nm indicated a clean one-to-one equilibrium between the native probe and the desilylated adduct, without involvement of intermediate species. Also, when the changes in absorbance at 460 and 392 nm bands were plotted against the concentrations of added fluoride ion, we witnessed a linear ratiometric regression with a good corelation coefficient (> 0.99) (Figure S5a). On the other hand, photoexcitation of compound 1 led to blue fluorescence with a vibronic emission spectrum.[30] Sharp bands observed at 442 nm and 467 nm, respectively, indicated the presence of monomeric emissive species in solution (Figure 2b). When the solution was exposed to TBAF, the intensity of the 442 nm band gradually decreased (~30-fold) with increasing analyte concentration, accompanied by the formation of a new red-shifted broad emission band centered at ~547 nm. Here also, we observed a ratiometric changes in emission response with respect of the concentration of added F^- ions (Figure S5b). This emission behavior can be attributed to the formation of a highly polarized ICT excited state associated with the desilylated phenoxide, which is further stabilized through intermolecular association and aggregation in the presence of the bulky tetrabutylammonium (TBA^+) counter-ion. The weakly coordinating and hydrophobic nature of TBA^+ facilitates loose ion pairing, allowing the phenoxide species to engage in π–π interactions and aggregate, thereby stabilizing the low-energy emissive state.[31] Consequently, the fluorescence color of the solution changed from blue to yellowish-orange. An isoemissive point at ~525 nm further supports the interconversion between two emissive species. To examine the specificity of the probe molecule toward the fluoride ion (TBAF), we also investigated the fluorescence response of compound 1 toward other commonly encountered anions (Figure 2c). No other tested anions, including basic ones such as CN^-, $H_2PO_4^-$, and AcO^-, showed any substantial change in the fluorescence spectra, and the blue fluorescence remained essentially unchanged. This observation highlights the requirement of a strong Si–F bond formation to initiate the sensing process. Considering the 1:2 interaction stoichiometry with compound 1, the binding constant with TBAF was calculated as 10.8 ± 0.04 (log K). The fluorescence titration studies also signified that the present system could detect fluoride ion as low as 0.621 μM from fluorimetric analysis. Interestingly, when compound 1 was treated with an equivalent amount of KF, only partial quenching of fluorescence intensity (~9.7-fold) was observed, which was significantly weaker than that induced by TBAF (Figure 2d). Notably, no new red-shifted emission band was detected even in the presence of excess KF. This contrasting behavior can be rationalized by the strong ion-pairing interaction between the phenoxide anion and the small, hard K^+ cation, which suppresses aggregation and limits excited-state ICT stabilization, thereby preventing the formation of the low-energy emissive species observed in the presence of TBAF.

Effect of microenvironment on fluoride ion-induced desilylation reaction: Further, we explored the effect of water content as well as pH of the medium on the extent of fluoride sensing. As the percentage of water (v/v) in the mixture medium was gradually increased from 0 to 100%, the degree of optical change induced by F^- ions decreased significantly (Figure 3a). This observation indicates that the sensing efficiency of compound 1 is strongly dependent on the polarity and solvation environment of the medium. In highly aqueous systems, fluoride ions experience extensive hydration, forming tightly bound solvation shells through strong hydrogen bonding interactions with water molecules.[32] The hydration energy of F^- ($-505\ kJ{\cdot}mol^{-1}$) is among the highest of all common anions, making the ion heavily

View Article Online
DOI: 10.1039/D6MA00118A

solvated and less available for nucleophilic attack on the Si–O bond of compound 1.[33] Consequently, in water-rich environments, the effective concentration of "free" or reactive fluoride decreases sharply, leading to reduced desilylation and a diminished spectral response. In contrast, in mixed organic–aqueous media such as DMF–H_2O (9:1, v/v), partial desolvation of fluoride occurs due to the lower dielectric constant and reduced hydrogen-bonding capacity of DMF. This partial desolvation enhances the nucleophilicity of F^-, facilitating its interaction with the silyl ether moiety of compound 1 and resulting in pronounced optical changes. In addition to solvent composition, the pH of the aqueous fragment in the DMF–H_2O mixture (with overall water content fixed at 10%, v/v) was also found to play a crucial role in dictating the extent of the response. A clear increase in absorbance at the characteristic charge-transfer band was observed under more basic conditions (Figure 3b). This pH dependence arises from the equilibrium between HF and F^- species in solution, where higher pH favors the deprotonated, nucleophilic fluoride form.[34] At lower pH, fluoride ions are protonated to form HF, which is far less reactive toward silicon centers and thus unable to induce desilylation. The enhanced response observed at higher pH therefore confirms that the sensing process relies on the availability of free F^- ions capable of attacking the silyl group.

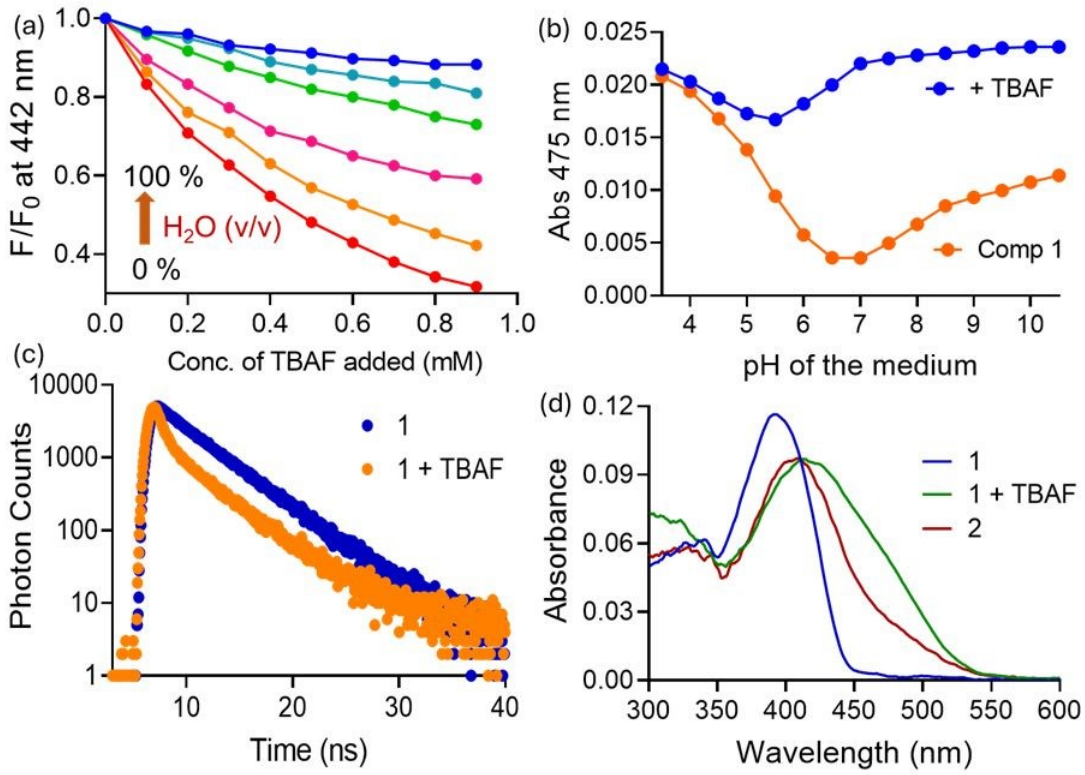

Figure 3. (a) Changes in fluorescence intensity of compound 1 (10 μM, λex = 390 nm) at 442 nm upon addition of TBAF (1 mM) in different DMF-H_2O medium (pH 7.5). (b) Changes in absorbance of compound 1 (10 μM) at 475 nm upon addition of TBAF (1 mM) in DMF-H_2O (9:1) at different pH conditions. (c) Changes in FL lifetime of compound 1 (10 μM, λex = 390 nm) at 550 nm with TBAF (1 mM) in DMF-H2O (9:1, pH 7.5 buffer) medium. (d) UV-visible spectra of compound 1 (10 μM, λex = 390 nm) with TBAF (1 mM) and compound 2 (desilylated product) in DMF-H2O (9:1, pH 7.5 buffer) medium.

Fluoride ion-induced modulation in charge transfer properties: Time-resolved fluorescence decay profiles recorded at the longer-emission wavelength revealed a marked decrease in the average lifetime of compound 1 upon addition of TBAF, compared to the native probe (Figure 3c). The faster decay in the presence of fluoride indicated the involvement of additional non-radiative deactivation pathways, consistent with fluoride-induced desilylation

View Article Online
DOI: 10.1039/D6MA00118A

and subsequent excited-state interactions. This lifetime shortening supported the formation of a highly polarized ICT state, which undergoes more rapid excited-state relaxation than the monomeric emissive species of compound 1. The FMO distributions indicate predominantly delocalized orbitals in the native state, corresponding to weak ICT, while desilylation induces electronic polarization rather than complete spatial separation, leading to an enhanced ICT character (Figure 4a). For the native compound 1, the HOMO was mainly localized over the conjugated aromatic backbone, while the LUMO was distributed over the comparatively electron-deficient core, indicating a weak intramolecular charge transfer (ICT) character upon excitation. In contrast, for the desilylated product, the HOMO orbitals were found to be significantly localized on the phenoxide-containing donor segment, reflecting the enhanced electron-donating ability after Si–O bond cleavage, whereas the LUMO remained delocalized over the π-conjugated backbone (Table S2). The largely delocalized HOMO and LUMO with minor spatial differentiation indicate weak ICT behavior. However, fluoride-induced desilylated phenoxide species improved orbital loclaization and enhanced electronic asymmetry, accompanied by a prominent increase in the dipole moment (2.1 D to 5.78 D), leading to partial ICT character, which is consistent with the observed red-shifted absorption and emission changes (Figure S9).

Fluoride ion-induced modulation in aggregation properties: Dynamic light scattering (DLS) measurements were performed to understand the aggregation behavior of compound 1 before and after exposure to TBAF (Figure 4b). In the absence of any fluoride source, compound 1 predominantly existed as monomeric or weakly associated species in solution, exhibiting a relatively small hydrodynamic diameter of 24.3 ± 3.5 nm, consistent with dispersed molecular entities in the DMF–H_2O (9:1) medium. Upon addition of TBAF, a pronounced increase in hydrodynamic diameter to 295.7 ± 12.8 nm was observed, clearly indicating the formation of larger supramolecular aggregates. This size expansion can be attributed to fluoride-triggered desilylation, which could generate a phenoxide anion with enhanced electron-donating character. The resulting anionic species, in the presence of the bulky and weakly coordinating tetrabutylammonium (TBA^+) counter-ion, undergoes loose ion pairing, enabling effective π–π stacking and intermolecular association. Such interactions promote the growth of extended aggregates rather than remaining as discrete molecular units. The aggregation behavior inferred from DLS is in good agreement with the photophysical observations, particularly the emergence of a red-shifted absorption band and a new low-energy emission band, which are characteristic of J-type aggregated states stabilized by enhanced ICT interactions. Further insight into the morphological evolution was obtained from field-emission scanning electron microscopy (FESEM). The FESEM images of pristine compound 1 showed relatively disordered and loosely packed morphologies (Figure 6a). In contrast, the TBAF-treated sample exhibited densely packed fibrous architectures, indicative of organized supramolecular self-assembly. The formation of such extended structures corroborates the DLS results and confirms that fluoride-induced desilylation not only modulates the electronic structure but also drives aggregation-assisted nanoscale reorganization.

Mechanistic insights into fluoride ion-induced desilylation reaction: The FT-IR spectra of compound 1 with and without TBAF revealed distinct and diagnostically meaningful changes. Compound 1 displayed characteristic absorptions attributable to the silyl protecting group, particularly prominent bands in the Si–O/Si–C stretching region (~1000–1150 cm^{-1}), along with associated alkyl vibrations (Figure 4c).[35] Upon interaction with TBAF, these bands were markedly attenuated or completely absent, accompanied by the appearance of a broad O–H stretching band in the 3200–3600 cm^{-1} region and noticeable intensity redistribution within the fingerprint region. These spectral transformations unequivocally indicated fluoride-induced desilylation reaction. Further, the ^{1}H-NMR spectra of compound 1 was recorded in

View Article Online
DOI: 10.1039/D6MA00118A

DMSO-d_6/D_2O (9:1) medium upon addition of both KF and TBAF (2 equiv.), respectively (Figure 5). The addition of fluoride showed shifting of peaks associated with tetra butyl silyl either functional group to the upfield region. Also, a new broad NMR peak was observed at ~5.6 ppm, indicating the presence of a hydroxyl functional group (Figure S6). While the overall spectral framework remains similar, distinct changes in peak positions, intensities, and broadening patterns are evident upon treatment with fluoride sources, particularly in the presence of TBAF. Compared to the parent compound, the spectrum recorded after the addition of TBAF exhibits pronounced peak broadening as well as intensity redistribution, whereas the spectrum obtained with KF shows comparatively minor perturbations. Also, the peaks that belong to terminal phenyl rings experienced upfield shifts upon analyte addition. These spectral differences can be rationalized by considering fluoride-induced desilylation and counter-ion–dependent ion-pairing and aggregation effects. Upon addition of TBAF, fluoride efficiently cleaves the silyl protecting group due to strong Si–F bond formation, generating a phenoxide anion. The bulky and weakly coordinating TBA^+ counter-ion forms loose ion pairs with the phenoxide species, allowing the anionic chromophores to interact freely through π–π stacking and intermolecular association.

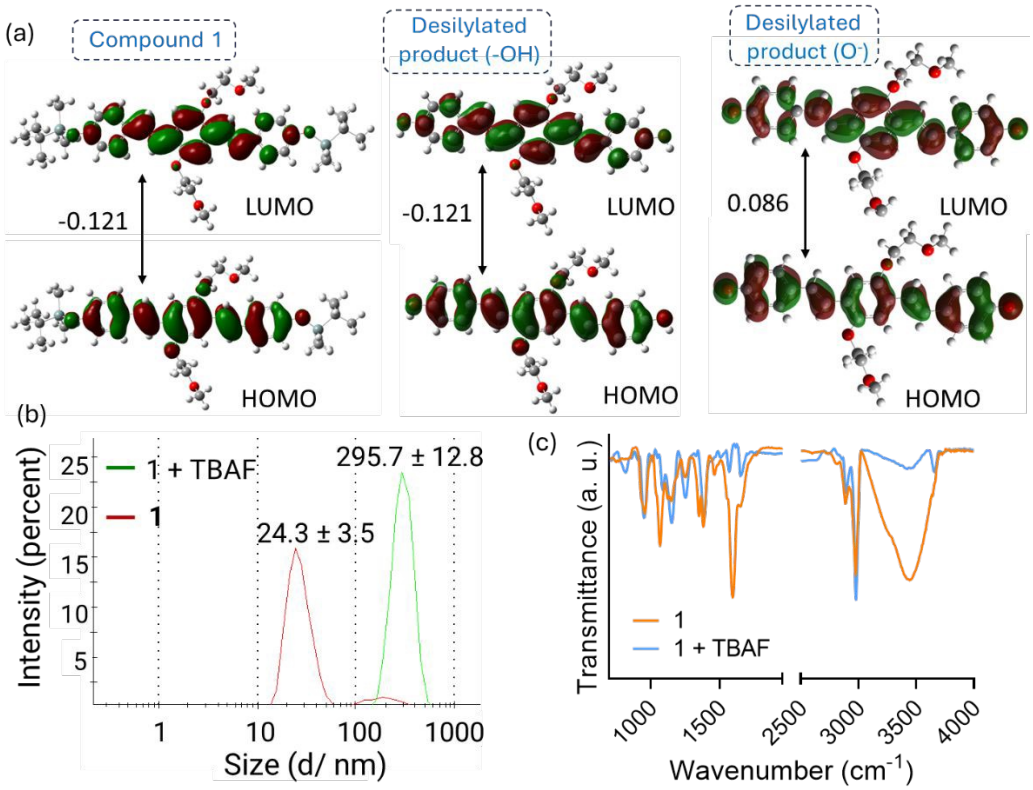

Figure 4. (a) Energy minimized structures of compound 1 and its corresponding desilylated products with FMO analysis (Energy gaps in a.u.). (b) Determination of average hydrodynamic diameters of compound 1 with and without TBAF in DMF-D_2O (9:1) mixture. (c) FT-IR spectra of compound 1 with and without TBAF.

Such aggregation and dynamic exchange processes result in peak broadening and changes in relative intensities, consistent with restricted molecular motion and multiple microenvironments in solution. These aggregation-induced effects are in line with the pronounced red-shifted absorption and new low-energy emission band observed in the photophysical studies. In contrast, when KF is used as the fluoride source, desilylation is significantly less efficient in the organic-rich solvent medium. Moreover, the smaller and harder K^+ cation forms tight contact ion pairs with the phenoxide oxygen, effectively stabilizing

discrete molecular species and suppressing intermolecular association.[36] As a result, the spectrum of the KF-treated sample shows only limited changes, primarily reflected as reduced intensity or minor shifts, without extensive broadening or formation of new spectral features.

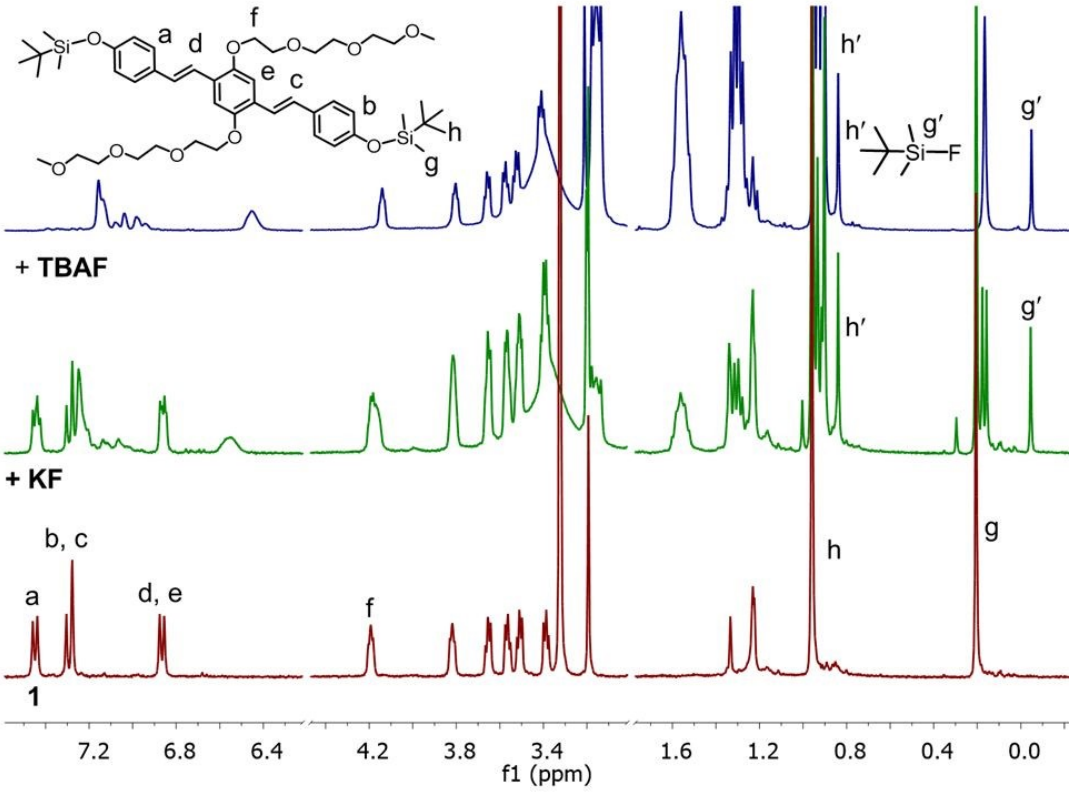

Figure 5. Partial ^{1}H-NMR spectra of 1 (5 mM) with KF and TBAF (2 equiv.) in DMSO-d_6/D_2O (9:1) medium. [inset shows the structure of compound 1 along with the concerned protons]

Further, to confirm the formation of the desilylated product in the reaction medium, we also compared the UV-visible spectrum of compound 1 (upon treatment with TBAF) with that of compound 2 containing terminal hydroxyl groups (Figure 3d). The hydroxyl functional group of compound 2 showed red-shifted absorption maxima as observed with compound 1, while treated with TBAF. This also confirms the TBAF-triggered desilylation in the reaction medium. The ESI-MS mass spectrum of 1 upon treatment with TBAF, showed a new base peak in additional to the original molecular ion peak (Figure S7). The newly appeared peak at 661.3 (m/z) could be assigned to the hydroxyl-ended desilylated product, formed during the nucleophilic attack by F^- ions. Further, to prove the nature of the fluoride interaction, we treated the solution of compound 1 + F^- with an equimolar amount of Ca^{2+} ions (Figure S8). The UV-visible spectral analysis of the mixture indicated that the addition of Ca^{2+} could not retrieve the absorption spectrum of the native compound, which indicated that the chemodosimetric interaction between compound 1 and TBAF was irreversible in nature.

Analysis of real-life samples for fluoride contents: To demonstrate the real-world applicability of compound 1 as a fluoride sensor, we evaluated its performance for estimating fluoride concentration in various natural water samples and further validated its response on solid-state paper-based strips.[37] The quantitative measurements were carried out in a DMF–H_2O (9:1, v/v) medium, where the corresponding water content was collected from the laboratory tap, pond and sea, respectively. Linear decrease in emission intensities at 442 nm emission band were observed with increasing fluoride concentration, following the Stern–

View Article Online
DOI: 10.1039/D6MA00118A

Volmer relationship (Figure 6d). The linear correlation ($R^2 > 0.99$) between fluorescence quenching and fluoride concentration confirms the reliability of the probe for analytical detection. Using this calibration, the lowest fluoride contents in different natural water samples were estimated in the range of 0.5–1.2 ppm, which are consistent with standard ion-selective electrode measurements. The quantitative analysis indicated recovery values lie within the range of 100 ± 3, with a standard deviation less than 5 % (Figure 6e). The high reproducibility and linearity of the optical response in these semi-aqueous media affirm that compound 1 can operate efficiently even in complex environmental matrices without interference from other common anions.

In addition to solution-based measurements, the sensing utility of compound 1 was further extended to a portable paper-strip format for rapid visual detection of fluoride. Filter paper strips were impregnated with a DMF solution of compound 1 (10^{-4} M) and subsequently air-dried.[7, 38] The FT-IR spectra of the pristine paper strips and the paper strips coated with compound 1 show distinct differences, confirming successful surface functionalization (Figure 6b). The uncoated paper exhibits characteristic cellulose bands, including broad O–H stretching in the 3200–3600 cm^{-1} region, C–H stretching near 2900 cm^{-1}, and strong C–O–C/C–O vibrations in the 1000–1150 cm^{-1} range.[39] Upon coating with compound 1, noticeable changes in band intensities and the appearance of additional absorptions are observed, particularly in the fingerprint region and the C–H stretching region, indicating the presence of organic functionalities from compound 1 on the paper surface. The partial attenuation and reshaping of the broad O–H band further suggest intermolecular interactions, such as hydrogen bonding, between the cellulose hydroxyl groups and compound 1. Upon exposure to aqueous fluoride solutions of varying concentrations, a distinct fluorescence color change was observed under UV illumination (λ_{ex} = 365 nm). The strips exhibited a progressive transition from bright blue to deep yellow with increasing fluoride concentration (Figure 6c). This visible fluorescence modulation arises from fluoride-induced desilylation of compound 1, forming the corresponding phenoxide species that promotes intramolecular charge transfer (ICT) and red-shifts the emission. The observed color gradient allows qualitative discrimination of fluoride levels even by the naked eye, making the system highly convenient for field deployment.

View Article Online
DOI: 10.1039/D6MA00118A

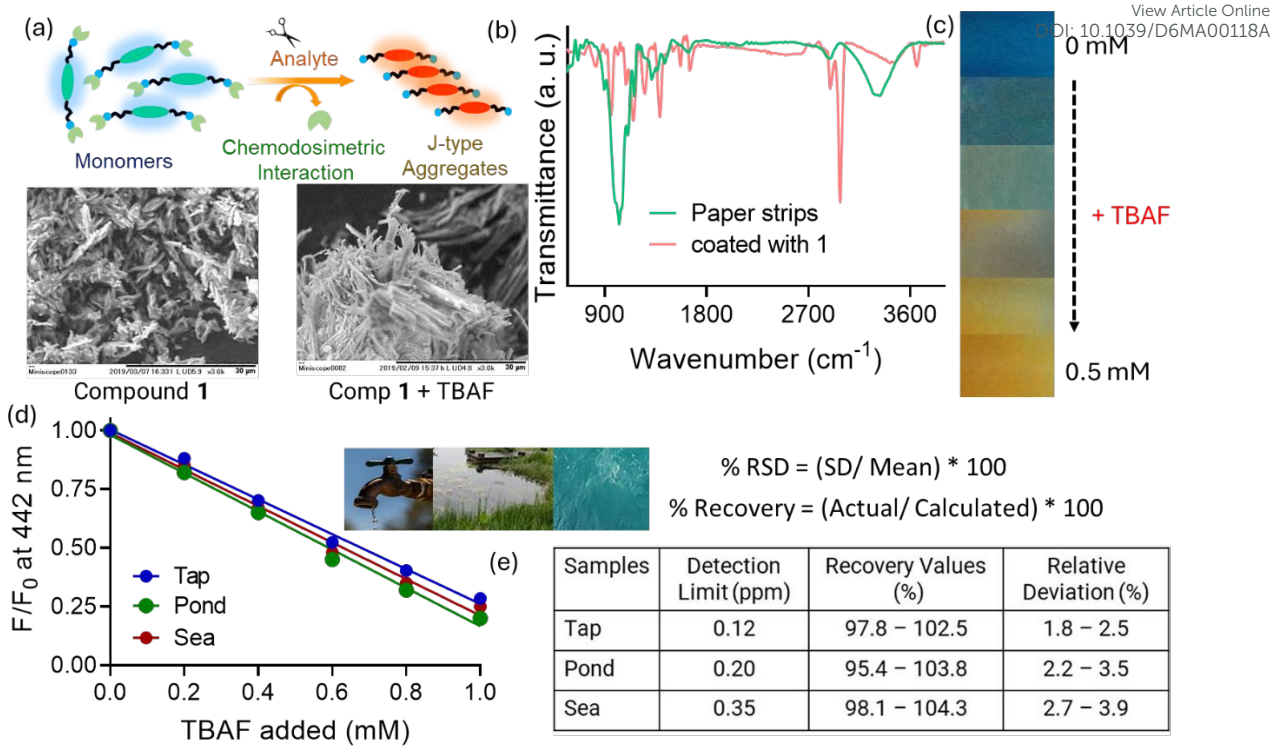

Samples	Detection Limit (ppm)	Recovery Values (%)	Relative Deviation (%)
Tap	0.12	97.8 – 102.5	1.8 – 2.5
Pond	0.20	95.4 – 103.8	2.2 – 3.5
Sea	0.35	98.1 – 104.3	2.7 – 3.9

Figure 6. (a) FESEM images of 1 with and without TBAF. (b) FT-IR spectra of cellulose paper strips with and without coating with compound 1. (c) Changes in FL color of compound 1 coated paper strips upon addition of TBAF (0 – 0.5 mM). (d) Changes in fluorescence intensity of 1 (10 μM, λex = 390 nm) at 442 nm upon addition of TBAF (0 - 25 μM) in DMF-H_2O (9:1, pH 7.4) mixture medium. (e) Quantification analysis of TBAF in different natural water samples.

Application to analysis of nerve gas agents: Considering the interaction of compound 1 towards fluoride ions in a semi-aqueous environment, we were intrigued to investigate its response towards various nerve gas agents, including Diisopropyl fluorophosphate (DFP).[40] However, unlike the previous experiment, here the buffer solution of pH 10 was used as the aqueous fragment. Such a basic pH was used for the spectroscopic studies to ensure the self-hydrolysis of DFP in the reaction medium, leading to the release of active analyte fluoride ions.[41] The choice of this basic environment stems from the earlier fluoride–response studies, where fluoride-induced desilylation was shown to play a pivotal role in modulating both the electronic and emissive properties of compound 1. At pH 10, DFP is known to undergo base-catalyzed cleavage of its P–F bond, generating F^-, which acts analogously to externally added fluoride reagents such as TBAF or KF (Figure 8a).[42]

Spectral response towards DFP in solution phase: Similar to TBAF, addition of DFP also resulted in a red-shifted absorption maximum, from 392 to 405 nm (Figure 7a). Visually, the color of the solution changes from bright greenish-yellow to a faint yellow. The titration studies showed a concentration-dependent increase in absorbance at the 450 nm band with concomitant quenching at the absorption maximum of the native compound. These features closely mirror the fluoride-triggered desilylation pathway, where cleavage of the Si–O bond leads to the generation of a phenoxide species, enhancing the ICT character of the probe molecule. The presence of an isosbestic-like behavior and linear correlation between absorbance ratios at 392 and 425 nm with increasing DFP concentration further confirmed a

View Article Online
DOI: 10.1039/D6MA00118A

clean equilibrium between the native and desilylated species. Such systematic spectral responses and visual color changes confirmed the fluoride-mediated interaction between compound 1 and DFP in the basic medium. At pH 10, DFP undergoes base-catalyzed hydrolysis to produce fluoride ions (F^-), which subsequently engage in desilylation reactions analogous to those initiated by TBAF or KF. This results in a similar bathochromic shift in the absorption profile due to increased ICT strength after the removal of the silyl protecting group. The bathochromic shift observed with DFP, although smaller than that induced by TBAF, suggests that the fluoride ions generated in situ are sufficient to initiate desilylation but are produced more slowly due to the gradual hydrolysis kinetics of DFP. Similarly, in the fluorescence mode, the addition of DFP led to quenching of the emission intensity at the 442 nm band (~2.9-fold) along with substantial spectral broadening and the appearance of a tail at the longer-wavelength region (Figure 7b). This emission behavior can be attributed to partial conversion of the silyl ether into the phenoxide form, producing mixed emissive states. The weaker fluorescence response observed with DFP compared to TBAF could be due to partial hydrolysis of DFP in the buffered medium, suggesting a relatively low effective concentration of fluoride ions. The lack of a new red-shifted emission band, as was seen in the case of TBAF, further implies limited aggregation and incomplete formation of the highly polarized ICT excited state that dominates the low-energy emission region in the presence of TBA^+ counterions.

A comparison of DFP vs TBAF in solution phase: To ensure this hypothesis, we followed the response of compound 1 towards DFP at neutral pH, i.e., in DMF–water (9:1, pH 7.0 buffer). Under these conditions, no detectable change in spectral response was observed, which clearly confirms that the presence of fluoride ions is essential for the observable optical response. When compound 1 was exposed to other chemical warfare agents (CWAs) under similar conditions, no change in fluorescence response was observed. Even other G-type nerve gas agents, such as DCNP or DCP, which are also susceptible to self-hydrolysis, did not induce any detectable optical change (Figure 7c).[43] This demonstrates that compound 1 selectively responds to fluoride-releasing agents and not to general phosphorous-based hydrolysis products. The strength of the signal attributed to DFP depends not only on the active concentration of fluoride ions but also on the kinetics of DFP hydrolysis. To further establish this, we monitored the time-course of the desilylation reaction both in the presence of TBAF (in DMF–H_2O 9:1, pH 7.5) and DFP (in DMF–H_2O 9:1, pH 10.5). The changes in absorbance at the 475 nm band, expressed as A/A_0, revealed that the desilylation reaction was extremely rapid with TBAF, reaching saturation within 2–3 minutes In contrast, the response with DFP was substantially delayed, requiring approximately 8–9 minutes to complete the spectral transformation (Figure 7d). This time lag directly reflects the slower fluoride generation from DFP hydrolysis compared to the instantaneous availability of fluoride in the case of TBAF. Collectively, these findings establish that compound 1 operates as a fluoride-responsive probe capable of reporting on the hydrolytic activity of fluoride-releasing nerve agents like DFP under basic aqueous conditions.

View Article Online
DOI: 10.1039/D6MA00118A

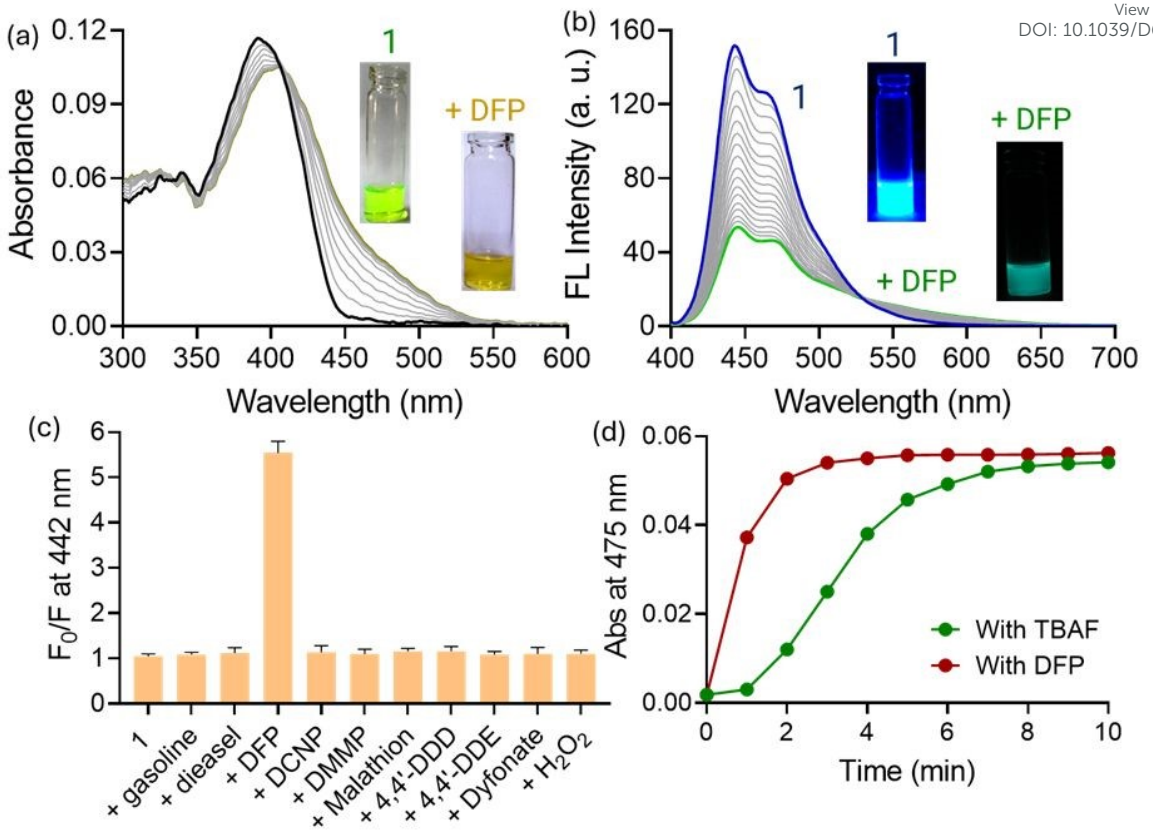

Figure 7. (a) UV-visible titration of 1 (10 μM) with DFP (0 – 1 mM) in DMF-H_2O (9:1, pH 10.5 buffer) medium. (b) Fluorescence titration of 1 (10 μM, λex = 390 nm) with DFP (0 – 1 mM) in DMF-H_2O (9:1, pH 10.5 buffer) medium. (c) Changes in fluorescence intensity of 1 (10 μM, λex = 390 nm) at 442 nm upon addition of various nerve agents (50 μM) in DMF-H_2O (9:1, pH 10.5 buffer) medium. (d) Changes in absorbance of 1 (10 μM) at 475 nm band upon addition of TBAF and DFP (50 μM) in DMF-H_2O (9:1) medium.

Mechanistic insights of DFP sensing in solution phase: To further validate the fluoride-induced desilylation mechanism proposed from the optical studies, the ^{1}H NMR spectra of compound 1 were recorded in DMSO-d_6/D_2O (9:1, with 10 mM Na_2CO_3/$NaHCO_3$) before and after treatment with DFP, respectively (Figure 8b). Interestingly, when compound 1 was treated with DFP, the resulting spectrum closely resembled that of the TBAF-treated sample, albeit with relatively weaker signal changes. The diagnostic disappearance of the silyl proton resonances and the upfield shift of the aromatic peaks confirmed that DFP, under basic conditions, effectively generates fluoride ions capable of promoting desilylation. However, the comparatively lower degree of broadening and smaller chemical-shifts suggested that the extent of conversion is limited, consistent with the partial hydrolysis of DFP in the pH 10 buffer medium.[44] This observation corroborates the weaker optical response and slower kinetics observed in the absorption and fluorescence studies, where DFP-induced desilylation required 8-9 minutes to reach completion, unlike the rapid reaction seen with TBAF. Taken together, these NMR results provide direct structural evidence for fluoride-mediated Si–O bond cleavage in compound 1, whether fluoride is introduced externally (TBAF) or generated in situ via hydrolysis of DFP.

View Article Online
DOI: 10.1039/D6MA00118A

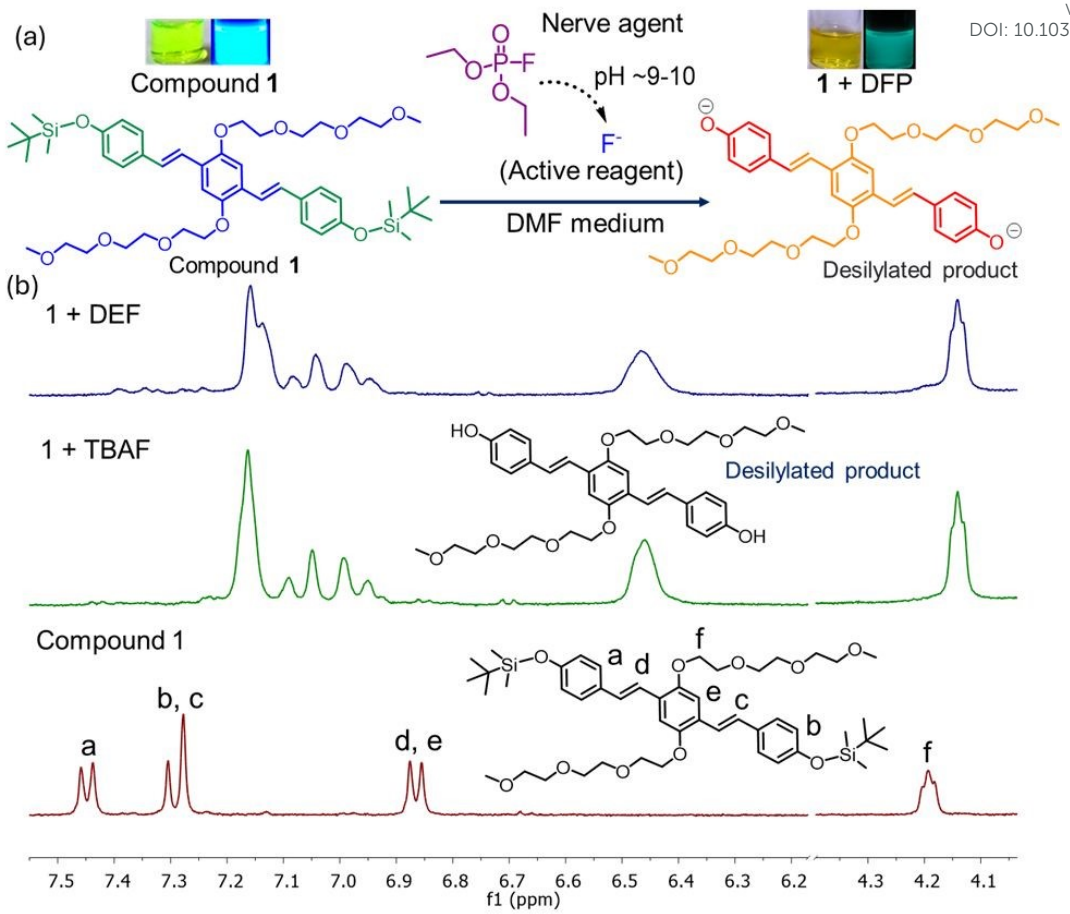

Figure 8. (a) Schematic diagram shows chemodosimetric response of 1 with in-situ generated F^- ions released from DFP. (b) Partial ^{1}H-NMR spectra of 1 (5 mM) with KF and TBAF (2 equiv.) in DMSO-d_6/D_2O (9:1) medium (with 10 mM Na_2CO_3/$NaHCO_3$). [Inset shows the structure of compound 1 along with the concerned protons]

CONCLUSION

In conclusion, we have synthesized a highly conjugated oligo polyvinylene compound with tert-butyldimethylsilyl ether functionalities. The oxyethylene chains improved aqueous compatibility and, therefore, better interaction with ionic analytes. The designed probe successfully demonstrated a highly efficient and selective fluoride-responsive molecular probe, capable of operating in semi-aqueous and mildly basic environments. The sensing mechanism involves fluoride-induced desilylation, wherein fluoride ions cleave the Si–O bond to form a phenoxide species possessing enhanced electron-donating character. This transformation significantly promotes the intramolecular charge transfer (ICT) character, resulting in a red-shifted absorption band and a characteristic fluorescence transition from blue to yellow. Spectroscopic and ^{1}H NMR analyses collectively confirmed the fluoride-triggered structural modification and the generation of a new low-energy emissive state. Theoretical FMO studies further supported this observation, showing increased electronic asymmetry and increased dipole moment (~2 to ~5.8 D) upon desilylation (in deprotonated state). The extent of fluoride response was found to be strongly influenced by both solvent composition and pH of the medium. Increasing water content attenuated the response due to extensive hydration of fluoride ions (ΔH_{hyd} = -505 kJ·mol^{-1}), which reduces their nucleophilicity and suppresses Si–O bond cleavage. In contrast, basic conditions favored free fluoride formation over HF, enhancing desilylation and promoting ICT modulation. The probe exhibited outstanding selectivity towards fluoride over other anions and performed reliably for fluoride

View Article Online
DOI: 10.1039/D6MA00118A

quantification in real water samples (0.5-1.2 ppm), consistent with ion-selective electrode results. Additionally, paper-based test strips coated with compound 1 enabled rapid on-site detection of fluoride through a distinct, visually perceptible fluorescence color change. Importantly, under controlled basic conditions, compound 1 also detected fluoride-releasing nerve agent simulants such as DFP, establishing its potential for dual-purpose applications in environmental monitoring, water safety analysis, and defence-related applications. This study thus provides both a mechanistic understanding and practical pathways for the design of next-generation fluoride-responsive optical sensors.

REFERENCES

1. Guerlin, A.; Dumur, F.; Dumas, E.; Miomandre, F.; Wantz, G.; Mayer, C. R., Tunable optical properties of chromophores derived from oligo (p-phenylene vinylene). *Org. Lett.* 2010, **12**, 2382–2385.
2. Shen, Q.; Song, G.; Lin, H.; Bai, H.; Huang, Y.; Lv, F.; Wang, S., Sensing, imaging, and therapeutic strategies endowing by conjugate polymers for precision medicine. *Adv. Mater.* 2024, **36**, 2310032.
3. Mateker, W. R.; McGehee, M. D., Progress in understanding degradation mechanisms and improving stability in organic photovoltaics. *Adv. Mater.* 2017, **29**, 1603940.
4. Goel, M.; Jayakannan, M., Supramolecular liquid crystalline π-conjugates: the role of aromatic π-stacking and van der Waals forces on the molecular self-assembly of oligophenylenevinylenes. *J. Phys. Chem. B* 2010, **114**, 12508–12519.
5. Ajayaghosh, A.; Praveen, V. K., π-Organogels of self-assembled p-phenylenevinylenes: soft materials with distinct size, shape, and functions. *Acc. Chem. Res.* 2007, **40**, 644–656.
6. Zhang, Y.; Qile, M.; Sun, J.; Xu, M.; Wang, K.; Cao, F.; Li, W.; Song, Q.; Zou, B.; Zhang, C., Ratiometric pressure sensors based on cyano-substituted oligo (p-phenylene vinylene) derivatives in the hybridized local and charge-transfer excited state. *J. Mater. Chem. C* 2016, **4**, 9954–9960.
7. Dey, N.; Bhattacharjee, S.; Bhattacharya, S., Addressing Multiple Ions Using Single Optical Probe: Multi-Color Response via Mutually Independent Sensing Pathways. *ChemistrySelect* 2020, **5**, 452–462.
8. Pise, S.; Dey, N., Modulation in the charge transfer characteristics of flexible bis-benzimidazole probes: independent sensing mechanisms for Hg 2+ and F−. *Dalton Trans.* 2025, **54**, 2896–2907.
9. Mujeeb, M. A.; Alam, M. Z.; Basha, H. A.; Afzal, S.; Khan, S. A., Synthesis, spectroscopic investigation of imidazole donor-π-acceptor chromophore: Opto-electronics and photonics properties in organized medium. *J. Mol. Struct.* 2025, **1341**, 142517.
10. Mujeeb, A.; Alam, M. Z.; Sultan; Aleem Basha, H.; Khan, S. A.; Afzal, S., Synthesis, physicochemical and third order nonlinear optical properties of bis-chalcone (BBDP) as donor-pi acceptor chromophore in organize medium. *J. Fluoresc.* 2025, **35**, 1393–1406.
11. Gotor, R.; Costero, A. M.; Gil, S.; Parra, M.; Martínez-Máñez, R.; Sancenon, F., A molecular probe for the highly selective chromogenic detection of DFP, a mimic of sarin and soman nerve agents. *Chem.–Eur. J.* 2011, **17**, 11994–11997.
12. Mondal, S.; Krishna, B.; Roy, S.; Dey, N., Discerning toxic nerve gas agents via a distinguishable 'turn-on'fluorescence response: multi-stimuli responsive quinoline derivatives in action. *Analyst* 2024, **149**, 3097–3107.
13. Fernandes, R. S.; Dey, N., Biodegradable Paper Sensor Functionalized with Oxidized Bisindolylmethane for Temporal Discrimination of Hazardous Organophosphorus Simulants in Aqueous Media. *Analyst* 2026.
14. Dey, N., Use of biocompatible natural product 'quinine'for naked-eye sensing of Sarin-surrogate both in solution-state and vapor phase. *J. Mol. Liq.* 2021, **327**, 114799.
15. Maurya, C. K.; Pathak, U.; Gupta, P. K., A dual-channel optical chemical sensing system for selective detection of nerve agent simulant DFP. *Anal. Bioanal. Chem.* 2021, **413**, 4501–4509.

View Article Online
DOI: 10.1039/D6MA00118A

16. Ugalde, G. A.; de Bairros, A. V., Determination of diethyl chlorophosphate for the recognition of organophosphorus chemical warfare agents. In *Sensing of Deadly Toxic Chemical Warfare Agents, Nerve Agent Simulants, and their Toxicological Aspects*, Elsevier: 2023; pp 97-109.
17. Purg, M.; Elias, M.; Kamerlin, S. C. L., Similar active sites and mechanisms do not lead to cross-promiscuity in organophosphate hydrolysis: implications for biotherapeutic engineering. *J. Am. Chem. Soc.* 2017, **139**, 17533–17546.
18. Yang, J.; Zhou, Y.; Kang, L.; Zhang, H.; Liu, C., A fluoride-responsive naphthalimide-derived chemosensor: Mechanistic insights into F--driven desilylation-decyanation cascade. *J. Fluor. Chem.* 2025, **283**, 110416.
19. Choudhury, A. R.; Dey, N., Molecular Amplification as an Affordable Strategy for Trace-Level Detection of Ionic Analytes with Fluorimetric or Colorimetric Readout. *ChemPhotoChem* 2023, **7**, e202200306.
20. Klingshirn, M. A.; Spear, S. K.; Subramanian, R.; Holbrey, J. D.; Huddleston, J. G.; Rogers, R. D., Gelation of ionic liquids using a cross-linked poly (ethylene glycol) gel matrix. *Chem. Mater.* 2004, **16**, 3091–3097.
21. Mandal, S. K.; Seth, P.; Kar, T., A stimuli-responsive l-DOPA-based supramolecular gel for the detection of fluoride ion. *New J. Chem.* 2024, **48**, 5429–5438.
22. Dey, N.; Jha, S.; Bhattacharya, S., Visual detection of a nerve agent simulant using chemically modified paper strips and dye-assembled inorganic nanocomposite. *Analyst* 2018, **143**, 528–535.
23. Han, J.; Kiss, L.; Mei, H.; Remete, A. M.; Ponikvar-Svet, M.; Sedgwick, D. M.; Roman, R.; Fustero, S.; Moriwaki, H.; Soloshonok, V. A., Chemical aspects of human and environmental overload with fluorine. *Chem. Rev.* 2021, **121**, 4678–4742.
24. Yagai, S.; Kubota, S.; Iwashima, T.; Kishikawa, K.; Nakanishi, T.; Karatsu, T.; Kitamura, A., Supramolecular Polymerization and Polymorphs of Oligo (p-phenylene vinylene)-Functionalized Bis-and Monoureas. *Chem.–Eur. J.* 2008, **14**, 5246–5257.
25. Wang, Y.; Liu, T.; Bu, L.; Li, J.; Yang, C.; Li, X.; Tao, Y.; Yang, W., Aqueous nanoaggregation-enhanced one-and two-photon fluorescence, crystalline J-aggregation-induced red shift, and amplified spontaneous emission of 9, 10-bis (p-dimethylaminostyryl) anthracene. *J. Phys. Chem. C* 2012, **116**, 15576–15583.
26. Precup-Blaga, F.; Garcia-Martinez, J.; Schenning, A.; Meijer, E., Highly emissive supramolecular oligo (p-phenylene vinylene) dendrimers. *J. Am. Chem. Soc.* 2003, **125**, 12953–12960.
27. Deng, Y.; Li, P.; Zhang, P.; Li, H., Deep-Blue Delayed Fluorescence Supramolecular Assembly with Ultrahigh Quantum Yields of 81% from an Extraordinary Source of π–π* Transition. *Adv. Opt. Mater.* 2022, **10**, 2101622.
28. Kwasniewski, S.; François, J.-P.; Deleuze, M., Effect of Thermal Motions on the Structure and UV− Visible Electronic Spectra of Stilbene and Model Oligomers of Poly (p-Phenylene Vinylene). *J. Phys. Chem. A* 2003, **107**, 5168–5180.
29. Dey, N.; Bhattacharya, S., Switchable optical probes for simultaneous targeting of multiple anions. *Chem.–Asian J.* 2020, **15**, 1759–1779.
30. Spano, F. C., Absorption and emission in pinwheel aggregates of oligo-phenylene vinylene molecules. *J. Chem. Phys.* 2001, **114**, 5376–5390.
31. Costa, T.; Garner, L. E.; Knaapila, M.; Thomas, A. W.; Rogers, S. E.; Bazan, G. C.; Burrows, H. D., Aggregation properties of p-phenylene vinylene based conjugated oligoelectrolytes with surfactants. *Langmuir* 2013, **29**, 10047–10058.
32. Buchner, R.; Wachter, W.; Hefter, G., Systematic variations of ion hydration in aqueous alkali metal fluoride solutions. *J. Phys. Chem. B* 2019, **123**, 10868–10876.
33. Zhan, C.-G.; Dixon, D. A., Hydration of the fluoride anion: structures and absolute hydration free energy from first-principles electronic structure calculations. *J. Phys. Chem. A 2004, **108**,* 2020–2029.
34. Sweeting, S. G.; Lennox, A. J., Non-Aqueous Binary and Ternary n HF· Base Fluoride Reagents: Characterization of Structure, Properties, and Reactivity. *J. Am. Chem. Soc. 2025.*

View Article Online
DOI: 10.1039/D6MA00118A

35. Vasin, A.; Rusavsky, A.; Kysil, D.; Prucnal, S.; Piryatinsky, Y. P.; Starik, S.; Nasieka, I.; Strelchuk, V.; Lysenko, V.; Nazarov, A., The effect of deposition processing on structural and luminescent properties of a-SiOC: H thin films fabricated by RF-magnetron sputtering. *J. Lumin.* 2017, **191**, 102–106.
36. Alabugin, I. V.; Kuhn, L.; Medvedev, M. G.; Krivoshchapov, N. V.; Vil, V. A.; Yaremenko, I. A.; Mehaffy, P.; Yarie, M.; Terent'ev, A. O.; Zolfigol, M. A., Stereoelectronic power of oxygen in control of chemical reactivity: the anomeric effect is not alone. *Chem. Soc. Rev.* 2021, **50**, 10253–10345.
37. Fernandes, R. S.; Dey, N., Bioinspired Composite Materials with Amplified Clusteroluminescence: Chemodosimetric Interaction Targeting Hypochlorite in Aqueous Medium. *ACS Mater. Au* 2024, **5**, 308–319.
38. Dey, N., Reversible color changing response of pyrenylated charge-transfer probes towards Hg 2+: linker-driven modulation of sensitivity and selectivity. *RSC Adv.* 2025, **15**, 9587–9593.
39. Ţucureanu, V.; Matei, A.; Avram, A. M., FTIR spectroscopy for carbon family study. *Crit. Rev. Anal. Chem.* 2016, **46**, 502–520.
40. Wymore, T.; Field, M. J.; Langan, P.; Smith, J. C.; Parks, J. M., Hydrolysis of DFP and the nerve agent (S)-sarin by DFPase proceeds along two different reaction pathways: implications for engineering bioscavengers. *J. Phys. Chem. B* 2014, **118**, 4479–4489.
41. Heiss, D. R.; Zehnder, D. W.; Jett, D. A.; Platoff Jr, G. E.; Yeung, D. T.; Brewer, B. N., Synthesis and storage stability of diisopropylfluorophosphate. *J. Chem.* 2016, **2016**, 3190891.
42. Kirby, A. J.; Medeiros, M.; Mora, J. R.; Oliveira, P. S.; Amer, A.; Williams, N. H.; Nome, F., Intramolecular general base catalysis in the hydrolysis of a phosphate diester. Calculational guidance to a choice of mechanism. *J. Org. Chem.* 2013, **78**, 1343–1353.
43. Abbas, Z.; Yadav, U.; Butcher, R. J.; Patra, A. K., Luminescent heteroleptic Eu (iii) probes for the selective detection of diethyl chlorophosphate as a G-series nerve agent mimic in the vapor phase using solid-state films. *J. Mater. Chem. C* 2021, **9**, 10037–10051.
44. Dumas, D. P.; Wild, J. R.; Raushel, F. M., Diisopropylfluorophosphate hydrolysis by a phosphotriesterase from. *Pseudomonas diminuta. Biotechnol. Appl. Biochem.* 1989**, *11***, 235-243.

Counter-Ion-Regulated Fluoride Sensing by a Silyl-Protected, Highly Conjugated Molecular Wire: From On-Field Analysis to Quantification of Nerve Gas Simulants

View Article Online
DOI: 10.1039/D6MA00118A

Prashant. D. Dewale, and Nilanjan Dey[a]*
[a]Department of Chemistry, Birla Institute of Technology and Science Pilani, Hyderabad campus, Hyderabad, Telangana 500078, India
Email: nilanjandey.iisc@gmail.com, nilanjan@hyderabad,bits-pilani.ac.in

Data will be available from authors on reasonable request